BAMS Article

Lead Isotopes in North American Precipitation Record the Presence of Saharan Dust

Sean R. Scott, Jason P. Dunion, Mark L. Olson, and David A. Gay

ABSTRACT: Atmospheric dust is an important mass transfer and nutrient supply process in Earth surface ecosystems. For decades, Saharan dust has been hypothesized as a supplier of nutrients to the Amazon rainforest and eastern North America. However, isotope studies aimed at detecting Saharan dust in the American sedimentary record have been ambiguous. A large Saharan dust storm emerged off the coast of Africa in June 2020 and extended into the southeastern United States. This storm provided a means to evaluate the influence of Saharan dust in North America confirmed by independent satellite and ground observations. Precipitation samples from 17 sites within the National Atmospheric Deposition Program (NADP) were obtained from throughout the southeastern United States prior to, during, and after the arrival of Saharan dust. Precipitation samples were measured for their lead (Pb) isotopic composition, total Pb content, and ^{210}Pb activity using multicollector inductively coupled plasma mass spectrometry. We measured a significant isotopic shift (approximately 0.7% in the ^{208}Pb/^{206}Pb relative to the ^{207}Pb/^{206}Pb) in precipitation that peaked in late June 2020 when the dust blanketed the southeastern United States. However, the magnitude and short time period of the isotopic shift would make it difficult to detect in sedimentary records.

KEYWORDS: Atmosphere; Africa; North America; Dust or dust storms

https://doi.org/10.1175/BAMS-D-20-0212.1
Corresponding author: Sean R. Scott, srscott4@wisc.edu
Supplemental material: https://doi.org/10.1175/BAMS-D-20-0212.2

In final form 25 August 2021

AFFILIATIONS: Scott—Wisconsin State Laboratory of Hygiene, University of Wisconsin–Madison, Madison, Wisconsin; **Dunion**—Cooperative Institute for Marine and Atmospheric Studies, University of Miami, and Hurricane Research Division, NOAA/Atlantic Oceanographic and Meteorological Laboratory, Miami, Florida; **Olson and Gay**—National Atmospheric Deposition Program, Wisconsin State Laboratory of Hygiene, University of Wisconsin–Madison, Madison, Wisconsin

Dust transport continuously blankets Earth, spreading nutrients across land and ocean surfaces, and affecting the composition and radiative heat budget of the atmosphere. The magnitude of dust transport and deposition varies through time; ice core records indicate glacial cycles control the overall atmospheric dust budget (Petit et al. 1981), while short-term variations result from seasonal weather patterns (Goudie 1983). Growing recognition of the importance of natural dust in Earth's biogeochemical cycles has resulted in numerous studies documenting continental and ocean basin scale transport across thousands of kilometers. For example, Asian dust is transported across the Pacific (Duce et al. 1980; Sassen 2002; Ewing et al. 2010) and regulates nutrient supply in the montane landscapes of the western United States (Aciego et al. 2017). Dust from Saharan Africa is distributed throughout the Mediterranean (Ganor and Mamane 1982), and across the Atlantic Ocean (Prospero and Carlson 1972; Chiapello et al. 1995), supplying nutrients to the Amazon basin (Swap et al. 1992; Yu et al. 2015), the Caribbean (Muhs et al. 1990; Kumar et al. 2018), and the eastern United States (Perry et al. 1997).

Detection, tracking, and predictions of modern dust sources and emissions rely on remote sensing (e.g., Washington et al. 2003; Baddock et al. 2009; Rayegani et al. 2020), climatic data (Tegen et al. 2004), and geochemical (Erel and Torrent 2010; Torfstein et al. 2017) and mineralogical (Schütz and Sebert 1987) indicators. Isotopes, especially radiogenic isotope ratios of strontium (Sr), neodymium (Nd), hafnium (Hf), and lead (Pb) may provide characteristic identification of dust sources (Grousset and Biscaye 2005; Aarons et al. 2017), although long distance transport can complicate isotopic systematics due to dust differentiation (i.e., preferential removal of heavier minerals/particulates as distance from the dust source increases; Aarons et al. 2013). Tracking of dust influence in distal regions is further complicated by mixing with local dust sources. Fortunately, local isotopic characteristics can be derived from precipitation (Graney and Landis 2013; Sherman et al. 2015) and in situ atmospheric aerosols (Bollhöfer and Rosman 2000, 2001) can provide a local atmospheric baseline composition that can be used to evaluate potential changes associated with dust influence, provided that the influence of distal dust or particle sources can be excluded. Nevertheless, evaluation of long-term trends of atmospheric deposition in a specific area can be challenged by complicated mixing relationships with local sources.

The Saharan Desert is the largest source of dust on Earth (Goudie 1983) with the Bodélé Depression being the most prominent source within the region (Goudie and Middleton 2001). Due to the influence of Saharan dust on Amazonian nutrient supply, Abouchami et al. (2013) sought to use Pb isotopic data to evaluate temporal changes in dust supply in the sedimentary record. In this study, Abouchami et al. (2013) compared isotopic compositions of source dust of the Bodélé Depression to Amazonian sediments, and they were unable to identify the Saharan dust signal presumably due to "consumption" of the dust by tropical weathering. Likewise, Escobar et al. (2013) did not detect the presence of a significant Saharan dust component in lake sediments in Florida. A study combining isotopic measurements with independent observations of the presence of Saharan dust transported across the Atlantic Ocean would therefore provide insight into the lack of isotopic evidence for Saharan dust influence in the sedimentary record.

In June 2020, a large Saharan dust storm was observed in satellite imagery, which showed the dust crossing the Atlantic Ocean and spreading throughout the Caribbean Sea, Gulf of

Mexico, and the southeastern United States. Ground based observations of red skies and poor air quality were reported throughout the region. This event provided a unique opportunity to utilize existing infrastructure of the National Atmospheric Deposition Program (NADP; see appendix A) to evaluate the presence of Saharan dust in atmospheric precipitation. Satellite observations were critical for coordination of sample collection, allowing for sampling sites to be targeted prior to arrival of the dust storm. The primary goal of this collaboration was to determine the effects of Saharan dust on the isotopic composition of atmospheric Pb deposition using preexisting NADP infrastructure.

Here, we present stable Pb isotopic composition, total Pb content, and ^{210}Pb activity data in precipitation samples from before, during, and after the arrival of Saharan dust across the southeastern United States (Fig. 1). These data allow for high-precision characterization of background atmospheric Pb isotopic compositions, which in turn allow for detection of an ephemeral signal associated with the Saharan dust storm. This study provides additional support for NADP as a rapid response network for atmospheric changes occurring at short time scales.

Constraints on the isotopic composition of North American atmospheric lead

Sedimentary records across the United States, as well as coral and oceanographic data, show that atmospheric Pb contents peaked in the 1970s and 1980s, but since the cessation of the use of leaded gasoline, atmospheric Pb concentrations have generally decreased (e.g., Eisenreich et al. 1986; Callender and Van Metre 1997; Kamenov et al. 2009; Kelly et al. 2009; Boyle et al. 2014; Zurbrick et al. 2018). Pb isotopic shifts in sediments correspond temporally to the use of leaded gasoline (Escobar et al. 2013), but are otherwise largely controlled by general industrial anthropogenic inputs since the start of the Industrial Revolution (Graney et al. 1995). While sedimentary records provide constraints on changes in atmospheric Pb isotope compositions through time, they can be complicated due to mixing of background atmospheric deposition of both local and distal point sources of pollution. Anthropogenic contamination sources carry a significant influence on isotopic composition and anthropogenic components can be separated from the natural "geogenic" background by chemical leaching (e.g., Shirahata et al. 1980; Hamelin et al. 1989; Kumar et al. 2014, 2018). However, sedimentary records do not provide a means to examine short-term excursions (on the order of days) in lead isotopic composition that have little leverage on the overall Pb budget.

The direct atmospheric Pb isotopic composition in North American has been evaluated in studies focused on aerosols (e.g., Bollhöfer and Rosman 2001), precipitation (e.g., Graney and Landis 2013; Sherman et al. 2015), and snowpack (Simonetti et al. 2000a,b). These datasets indicate that the primary sources of today's atmospheric Pb are derived from industrial activities, smelting, and coal burning (Graney and Landis 2013; Sherman et al. 2015). Isotopic datasets, either in the sedimentary record, precipitation, and/or aerosols, show that atmospheric Pb isotopic composition is not a single point, but rather an isotopic trend that varies across the landscape due to changes in proximity to different industrial sources.

The North American atmospheric trend line

In many cases, datasets of atmospheric Pb composition have been produced by either single-collector inductively coupled plasma mass spectrometry (ICPMS) (Graney and Landis 2013; Sherman et al. 2015) or multicollector thermal ionization mass spectrometry (TIMS) (Bollhöfer and Rosman 2000, 2001); however, a high-precision analysis using multicollector inductively coupled plasma mass spectrometry (MC-ICPMS) of direct atmospheric Pb composition is lacking. In this study we used a NeptunePlus MC-ICPMS with an Aridus 3 desolvating nebulizer system to enhance sensitivity, allowing us to produce high-precision isotopic data on relatively low total Pb quantities (as low as 12 ng; see appendix B for methods).

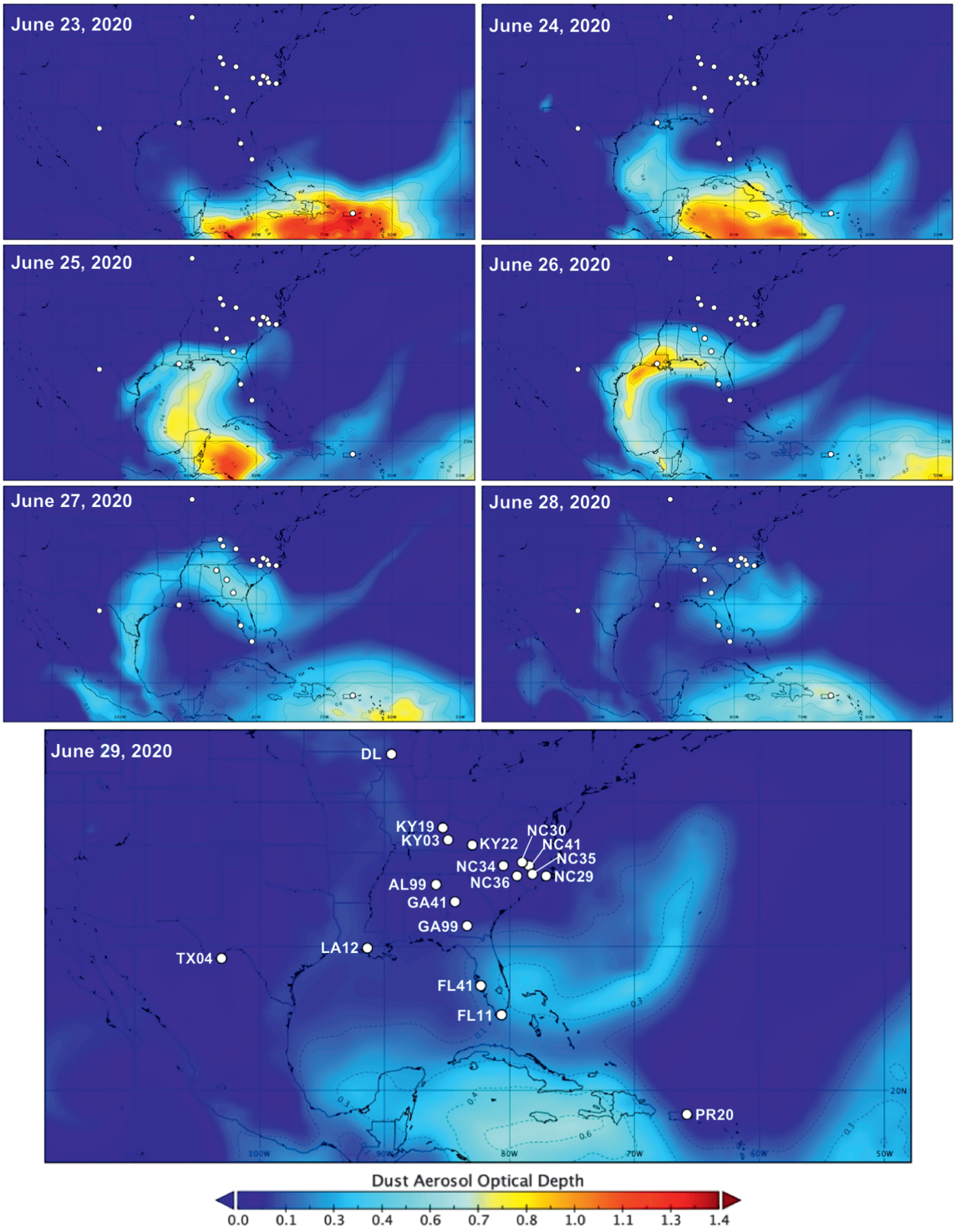

Fig. 1. Dust aerosol optical depth from 23 to 29 Jun 2020 from the Navy Aerosol Analysis and Prediction System (NAAPS). Weekly sample collection of precipitation from this interval occurred on 30 Jun 2020. All sites contained Pb isotopic evidence for Saharan dust influence as indicated by the median Δ208/206 value of 0.0068 (see text for explanation). Sites shown on the 29 Jun 2020 image correspond to the sample sites in the data table in the online supplement (https://doi.org/10.1175/BAMS-D-20-0212.2). DL = Devil's Lake, Wisconsin.

Pb isotopic compositions of the precipitation samples have generally comparable compositions to previous North American sample sets (Fig. 2). However, the relatively high $^{208}Pb/^{206}Pb$ in some samples tend toward dust compositions that closely resemble residual particulate compositions measured in Cape Verde aerosols during summer incursions of the Saharan air layer (Kumar et al. 2018). Deviations in precipitation Pb isotopic composition are correlated to

independent observations of Saharan dust spreading across the sampling area, motivating a more precise evaluation of the timing and magnitude of these isotopic deviations.

Using our high-precision Pb isotope data in samples collected prior to the arrival of the Saharan dust storm, we establish the North American atmospheric trend line (NATL), and argue that deviations from this trend line are the result of non–locally produced atmospheric dust inputs in our dataset. This approach is similar to that of Hart (1984), who established the "Northern Hemisphere reference line" to discriminate between compositionally variable midocean ridge basalts, and has also been applied in studies of external atmospheric influences in snow layers (e.g., Bory et al. 2014). In the case of the NATL, high-precision Pb data are critical for evaluating changes in atmospheric composition. Pb isotopic compositions from the same sample locations are not necessarily the same through time, but should lie on the same trend line during time periods of predominately local dust inputs to the atmosphere. The equation for the NATL reference line is

$$^{208}\mathrm{Pb}/^{206}\mathrm{Pb}_{\mathrm{NATL}} = 1.6665\left(^{207}\mathrm{Pb}/^{206}\mathrm{Pb}\right) + 0.6616. \quad (1)$$

The vertical deviation along the y axis from this line can be used to determine external atmospheric inputs in the measured $^{208}\mathrm{Pb}/^{206}\mathrm{Pb}$ of a sample ($^{208}\mathrm{Pb}/^{206}\mathrm{Pb}_{\mathrm{M}}$), e.g., from Saharan dust, expressed in delta notation as

$$\Delta 208/206 = {}^{208}\mathrm{Pb}/^{206}\mathrm{Pb}_{\mathrm{M}} - {}^{208}\mathrm{Pb}/^{206}\mathrm{Pb}_{\mathrm{NATL}}. \quad (2)$$

This metric can then be used to evaluate the presence of foreign atmospheric inputs through time. The Δ208/206 value should be nearly zero when only local dust sources are present in the atmosphere, whereas this number should deviate from zero in the presence of foreign dust inputs. Isotopic compositions of Saharan dust samples collected from Cape Verde showed that particulates from Saharan dust storms contain components of both anthropogenic and geologically derived Pb. The NATL trends toward the anthropogenic components documented by Kumar et al. (2018), while the geological components sit above the NATL in Fig. 2. Therefore, the Δ208/206 value is positive when geologically derived Saharan dust is present in the North American atmosphere.

Impact of Saharan dust

Calculated Δ208/206 through time for the southeastern U.S. precipitation samples reveal a characteristic shift in Pb isotopic composition associated with Saharan dust (Fig. 3). Samples with end collection dates of 16 and 23 June 2020 have Δ208/206 less than 0.002, with the exception of one sample from Big Bend, Texas (site TX04; 23 June 2020), and a sample from El Verde, Puerto Rico (site PR20; 23 June 2020). These earlier arrival times are consistent with Satellite observations from the NASA Suomi National Polar-Orbiting Partnership satellite system (www.nasa.gov/feature/goddard/2020/nasa-noaa-s-suomi-npp-satellite-analyzes-saharan-dust-aerosol-blanket) showing that these two sites were under the spreading Sahara dust in the atmosphere earlier in the sampling period than the other sites. These samples reflect isotopic ratios in this first week consistent with ratios influenced by the Saharan dust and seen at all other sites in the next 7-day period. The sampling operator noted the presence of "dense desert dust" over Puerto Rico during this collection date, providing observational confirmation of the influence of Saharan dust on the atmospheric Pb isotopic composition. Desert dust was not noted in the Texas sampling data; however, the total Pb content of the Texas sample was approximately an order of magnitude greater than the median Pb content for all samples (1.12 ng g^{-1} vs a median of 0.075 ng g^{-1}).

During the primary influx of Saharan dust across the southeastern United States, Δ208/206 values were higher relative to values from the previous sampling intervals. For sampling

intervals ending on 30 June 2020, Δ208/206 values ranged from 0.0031 at site AL99 to 0.0218 at site PR20, with a median value of 0.0068. In the week after the peak (end collection dates of 7–8 July 2020), some sites returned to predust compositions while others maintained some degree of elevated Δ208/206 up to 0.0064 in FL41, with a median value of 0.0029. These data show that the maximum influence of Saharan dust occurred during the sampling interval from 23 to 30 June 2020, and that the peak of Saharan dust impact is relatively short, probably spanning less than 2 weeks.

Unlike the isotopic compositions, total Pb content and ^{210}Pb activities generally did not change across the southeastern United States during the peak of Saharan dust influence. There were two exceptions, one being the TX04 (1.12 ng g^{-1} Pb) sample with an end collection date of 23 June 2020, and the PR20 sample (0.306 ng g^{-1} Pb) with an end collection date of 30 June 2020. These elevated total Pb contents also correspond to higher ^{210}Pb activities. Excluding these samples, ^{210}Pb activities ranged from 0.014 to 0.129 Bq kg^{-1}, and are generally consistent with ^{210}Pb activities in precipitation (e.g., Settle et al. 1982). These data indicate that while the Saharan dust impacted the stable Pb isotopic composition, it did not have a significant impact on the Pb content or ^{210}Pb activity of the atmosphere. This lack of impact on the total and radioactive Pb components of the atmosphere is consistent with the largely geological origins of Saharan dust suggested in recent isotopic studies of North Atlantic dust sources (e.g., Conway et al. 2019), and shown isotopically when comparing our dataset to the isotopic compositions of residual particulate components from Kumar et al. (2018).

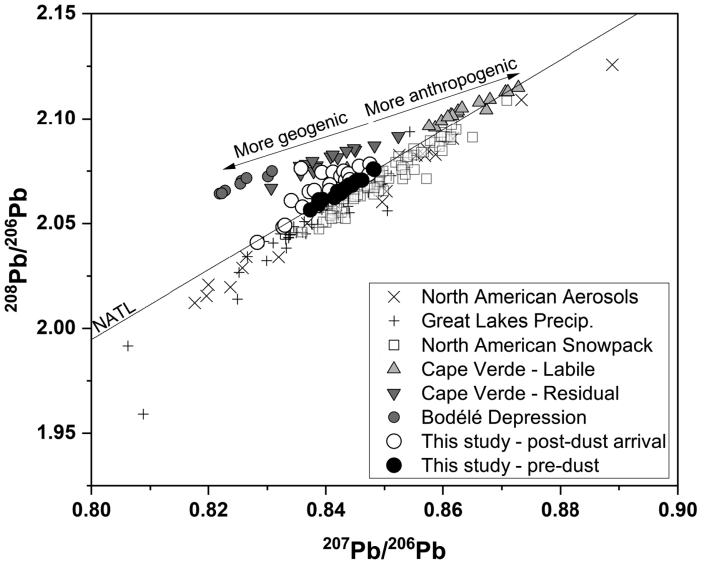

Fig. 2. Diagram showing the trend line for ^{208}Pb/^{206}Pb vs ^{207}Pb/^{206}Pb for North American atmospheric samples and Saharan dust source samples. Isotopic trends result from mixing of various geogenic and anthropogenic sources that vary depending on the sampling region, sources that can be distinguished by chemical processing procedures (e.g., Kumar et al. 2018). The labile component reflects anthropogenic Pb, whereas the residual component is what remains after the labile component has been removed by acid leaching. Foreign geogenic atmospheric inputs, such as dust from the Bodélé Depression or other geogenic Saharan dust sources, cause a deviation in atmospheric Pb isotopic composition away from typical North American atmospheric compositions. The North American atmospheric trend line (NATL) used in this study is shown for reference, and intersects the anthropogenic component represented by the labile Pb ratios in Cape Verde aerosols collected during a Saharan air layer incursion. Data sources: North American aerosols (Bollhöfer and Rosman 2001), Great Lakes precip. (Sherman et al. 2015), North American snowpack (Simonetti et al. 2000a,b), Cape Verde (Kumar et al. 2018), Bodélé Depression (Abouchami et al. 2013).

The lack of significant change in the total Pb flux due to this Saharan dust event provides insight into observations made in previous studies aimed at detecting such dust influence using Pb isotopes in sedimentary records. This dust storm influenced the southeastern U.S. sites for approximately 2 weeks, accounting for about 4% of the yearly Pb budget, with an associated isotopic shift of ~0.7% (i.e., median Δ8/6 = 0.0068). These basic metrics, along with the frequency of storms of this magnitude, suggests that an isotopic signal for Saharan dust would be difficult to detect in the sedimentary record. Even if the depositional system is able to preserve the dust in place (e.g., in lake sediments), the isotopic leverage of this dust is unlikely to have a significant impact on the isotopic compositions preserved in the sedimentary record consistent with observations by Abouchami et al. (2013) in the Amazon and Escobar et al. (2013) in Florida. Therefore, soil/sediment studies of dust impacts using Pb isotopes are unlikely

to provide a robust metric of dust influence in these landscapes. Given the recognized importance of atmospheric dust transport throughout Earth's history, we argue that Pb isotopes are best suited to detect short-term atmospheric changes in "real-time" samples, and additional chemical and isotopic parameters are necessary for detecting dust components in the sedimentary record.

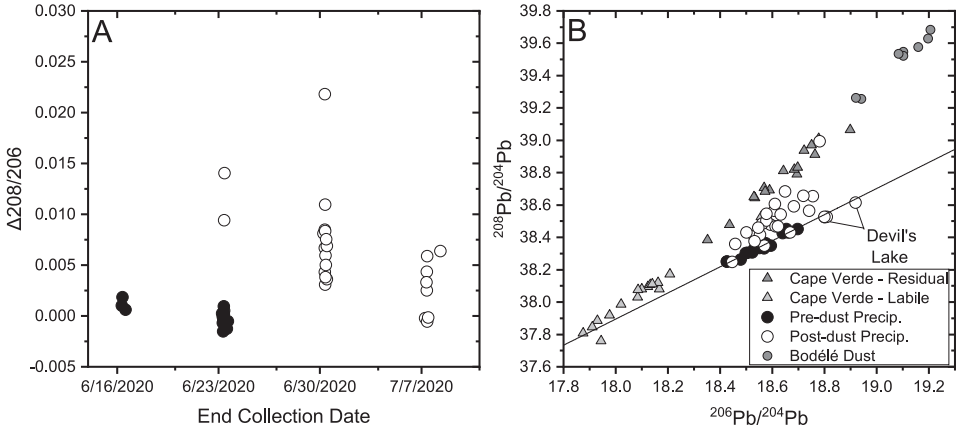

Fig. 3. Isotopic shift in precipitation samples due to influence of Saharan dust as recorded by the Δ208/206 value. (a) Diagram showing Δ208/206 vs the end collection date over week-long sampling intervals. The filled black circles indicate samples used to calculate the NATL measured in southeastern U.S. precipitation prior to arrival of the Saharan dust. The peak of dust influence occurred in the sampling interval from 23 to 30 Jun 2020, where all samples deviated to higher Δ208/206. (b) $^{208}Pb/^{204}Pb$ vs $^{206}Pb/^{204}Pb$ for samples in this study, Cape Verde aerosol samples collected during a Saharan dust incursion during summer 2013 split into the labile (anthropogenic) and residual (geologic) portions by acid leaching (Kumar et al. 2018), Bodélé Depression dust (Abouchami et al. 2013), and the NATL. The solid line is a linear regression fit to the same samples used to calculate the NATL for $^{208}Pb/^{206}Pb$ vs $^{207}Pb/^{206}Pb$. Devil's Lake was sampled for quality control purposes and falls on the NATL, consistent with its endorheic characteristics.

Summary

Atmospheric dust storms are responsible for significant mass transfer across Earth's surface, but efforts to detect an isotopic dust signal in the sedimentary record have been ambiguous. In this study, we took advantage of a large Saharan dust storm that crossed the Atlantic Ocean and blanketed the southeastern United States. Rapid response and coordination with NADP helped establish a predust background, which was then used to detect an isotopic shift in precipitation samples collected when the Saharan dust arrived. This shift lasted for ~2 weeks and did not cause changes in total Pb content, likely due to the primarily geological source of the dust. The relatively low flux of Pb suggests that dust storms of this frequency and magnitude would have little leverage on the sedimentary isotopic record. However, we did detect a shift in the Pb isotopic composition (indicated by a change in the $^{208}Pb/^{206}Pb$ relative to the $^{207}Pb/^{206}Pb$, referred to as the Δ208/206) consistent with previously published data on geologically sourced Saharan dust. This study also provides further support for utilizing NADP infrastructure to detect rapid, short-term changes in atmospheric conditions. Longer-term studies using NADP infrastructure that utilize isotopic composition data over longer time periods could provide a more quantitative analysis of the total quantities of dust being deposited over a given area. In addition, such studies could document ongoing changes in dust flux associated with changing climate and weather patterns that are expected to occur in the future.

Acknowledgments. We thank the staff of the National Atmospheric Deposition Program (http://nadp.slh.wisc.edu/), specifically Amy Mager, for quickly reacting to requests for sample preservation. Wafa Abouchami, as well as two anonymous reviewers, provided critical feedback that greatly improved the quality of the manuscript.

Appendix A: National Atmospheric Deposition Program

NADP was organized by the U.S. State Agricultural Experiment Stations as a precipitation chemistry monitoring network in 1977, and has expanded over time to include several networks of monitoring stations that provide atmospheric deposition data across the United States. The largest grid is the National Trends Network (NTN) operating 263 sites that provide long-term records of precipitation chemistry away from urban areas and point sources of pollution. Samples are collected weekly, with a wet deposition only system that opens to a bucket collector during precipitation events. One exception is the PR20 site that also collected some dry deposition during the sampling period (i.e., the bucket was open to the atmosphere continuously). Samples are transferred in the field to low-density polyethylene (LDPE) containers cleaned at the Central Analytical Laboratory (CAL) housed at the Wisconsin State Laboratory of Hygiene (WSLH). On arrival at the CAL, aliquots are transferred for the primary NTN analyses and separate aliquots are stored in the sample archive. Excess precipitation was set aside for analyses in this study. NADP transferred from the University of Illinois to WSLH in 2018.

NADP is well suited for detection of atmospheric events due to its spatial coverage. Previous efforts to identify short-term atmospheric anomalies include the detection of fission products after the Fukushima Dai-ichi Nuclear Power Station incident of 12 March 2011 (Wetherbee et al. 2012).

Appendix B: Analytical methods

The primary goal of the analytical methods used for this study were to detect an atmospheric signal while minimizing the complexity of sample processing procedures. To achieve this goal, the excess precipitation samples set aside from the NADP NTN were transferred to the Trace Elements Clean Laboratory (TECL) at WSLH in their primary 1-L Nalgene LDPE sample bottles. To resuspend any dust that had settled on the bottoms of the containers, samples were shaken, then transferred gravimetrically to cleaned 1-L Teflon perfluoroalkoxy alkane (PFA) jars. Total sample weights ranged from ~200 to 950 g. The samples were then taken to dryness over ~2 days on a hotplate at 110°C in a high-efficiency particulate air (HEPA)-filtered laminar-flow hood. To assess any possible contamination from the long drying period, empty 1 L PFA jars were placed in the hood during the drying procedure and treated as unknowns. Cleaned NADP sampling bottles were also tested for Pb contamination by filling bottles with 18.2 MΩ cm H_2O, sitting for approximately 4 days, then transferring the H_2O to 1-L PFA jars and taken to dryness.

Reference materials with comparable matrices were not available, and we opted to collect two separate lake water samples from Devil's Lake, Wisconsin, in 2-L PFA bottles for an assessment of quality control for Pb isotopic compositions. Devil's Lake was chosen because it is endorheic, suggesting that its isotopic composition should reflect local atmospheric signals. The Devil's Lake samples were treated as unknowns using the same procedures as those used for the precipitation samples. We also used National Research Council–Canada reference material SLRS-6 (river water) for quality control for the total Pb contents measured by isotope dilution. Approximately 5-mL aliquots of SLRS-6 were weighed into 23-mL PFA jars for this purpose. All samples were processed using Optima Grade acids and Type 1 (18.2 MΩ cm) H_2O.

After drying, samples were redissolved in 9.9 mL of 16-M HNO_3 and 0.1 mL of 29-M HF. One milliliter of this sample solution was transferred to a separate 23-mL PFA jar, and spiked with a known quantity of ^{206}Pb isotopic tracer for isotope dilution analysis (along with the SLRS-6 aliquots). The isotope dilution aliquot and remaining 9-mL bulk sample (isotopic composition aliquot) were both dried, then redissolved in either 0.6 mL of 1-M HBr (isotope dilution) or 1.8 mL of 1-M HBr (isotopic composition) for Pb purification after Strelow and Torien (1966). Sample solutions were loaded onto BioRad Polyprep columns containing 0.6 mL of previously cleaned AG1-X8 anion exchange resin conditioned in 1-M HBr. After loading, the bulk sample

matrix was eluted using washes of 0.6, 1.2, 1.2, and 4.8 mL of 1-M HBr. Pb was collected in previously cleaned 15-mL PFA jars using two 0.6-mL washes of H_2O, followed by two 3.6-mL washes of 1-M HNO_3. Purified Pb solutions were dried, then redissolved in 2% (0.5-M) HNO_3 in preparation for isotopic analysis using MC-ICPMS.

All isotopic analyses were performed on the NeptunePlus MC-ICPMS (Thermo Fisher Scientific Inc., Waltham, Massachusetts) housed in the TECL at WSLH. Samples were introduced into the plasma in 2% HNO_3 using an Aridus 3 desolvating nebulizer system (Teledyne Cetac) with the Jet sampler cone and X skimmer cone configuration. Three isotopic measurements were completed for each sample. The first analysis used the unspiked samples to measure the stable Pb isotopic composition. Thallium (Tl) was added to each sample to correct for mass bias using the exponential fractionation law and assuming $^{205}Tl/^{203}Tl = 2.387$. The ^{206}Pb, ^{207}Pb, and ^{208}Pb were measured on the high 1, high 2, and high 3 Faraday cups, respectively, and ^{204}Pb was measured on the low 1 Faraday cup. ^{205}Tl was measured on the center Faraday cup, and ^{203}Tl was measured on the low 2 Faraday cup. The low 3 Faraday cup was used to monitor for Hg interferences by measuring the ^{202}Hg isotope. Isotope ratios were measured in static mode for 60 cycles of 8-s integrations. The international Pb reference material NBS981 was measured periodically, and final isotope ratios are reported relative to NBS981 values of Thirlwall (2002). Final analyte concentrations were 10 ppb Pb + 3 ppb Tl. All samples and NBS981 standards were corrected for on-peak baselines by measuring a blank 2% HNO_3 solution before every sample and standard analysis. One bottle of the Devil's Lake water gave $^{208}Pb/^{206}Pb = 2.0490 \pm 0.0010$ and $^{207}Pb/^{206}Pb = 0.8329 \pm 0.0004$ (2 std dev, $n = 3$). A second bottle of Devil's Lake water was analyzed once, and gave $^{208}Pb/^{206}Pb = 2.0412$ and $^{207}Pb/^{206}Pb = 0.8283$, a value distinct from the first bottle. These samples were unfiltered, and their variations likely reflect different proportions of unfiltered solids present in the lake water. However, both samples have Δ208/206 within 0.001 of the NATL, consistent with local atmospheric origins.

The second analysis used the spiked samples to measure the $^{208}Pb/^{206}Pb$ ratio for the isotope dilution calculation for total Pb content. The procedure was similar to that used for the stable isotopic composition measurements (i.e., Tl-normalization and seven Faraday collectors), except samples were analyzed for 30 cycles of 4-s integrations. The NBS981 standard was measured before and after every sample (sample-standard bracketing), and the final $^{208}Pb/^{206}Pb$ ratio for the isotope dilution calculation was normalized to the NBS981 value of Thirlwall (2002). Final analyte concentrations were 1–5 ppb Pb + 1 ppb Tl. All samples and NBS981 standards were corrected for on-peak baselines by measuring a blank 2% HNO_3 solution before every sample and standard analysis. Results for SLRS-6 gave 0.173 ± 0.003 ng g^{-1} Pb (1 std dev, $n = 4$), consistent with the certificate value of 0.170 ± 0.026 μg L^{-1}. Results for the three analyses of one bottle of Devil's Lake water were 0.030 ± 0.001 ng g^{-1} Pb (1 std dev, $n = 3$). The second bottle was measured at 0.019 ng g^{-1} Pb, confirming the heterogeneity of the unfiltered lake water indicated by the isotopic compositions.

The third analysis used the remaining unspiked sample solutions to measure the $^{210}Pb/^{208}Pb$ ratio for calculation of the ^{210}Pb activity. The analytical procedure followed methods described in Scott et al. (2019); the central secondary electron multiplier/retarding potential quadrupole (SEM/RPQ) was used to measure the ^{210}Pb beam and the low 2 Faraday cup was used to measure the ^{208}Pb. Small remaining sample volumes prevented direct measurement of the ^{208}Pb tail on ^{210}Pb. Instead, samples were corrected for tailing of ^{208}Pb onto ^{210}Pb by measuring the abundance sensitivity at 2 amu (55 ppb) in an NBS981 standard and using this to correct the ^{210}Pb counts based on the ^{208}Pb intensity in each sample. Prior to the analyses, a ^{234}U beam was used to calculate the transmission factor for the RPQ. $^{210}Pb/^{208}Pb$ ratios were measured in static mode for 10 cycles of 4-s integrations. All samples were corrected for on-peak baselines using a blank 2% HNO_3 solution. The final ^{210}Pb activity was calculated using the stable Pb isotopic composition and total Pb content measured by isotope dilution. Scott et al. (2019)

estimated uncertainties for this method at ~30% due to the large tail corrections and uncertainty in transmission. The standard deviation of three measurements of one bottle of Devil's Lake water was ~8.0% for the final ^{210}Pb activity in Bq kg^{-1}.

Procedural and bottle testing blanks were analyzed for Pb contents and isotopic compositions; however, Pb blanks did not provide sufficient material for an accurate measurement of the blank Pb isotopic composition. Total procedural blanks that included the blank PFA jar drying procedure amounted to <14 picograms (pg) of Pb (n = 5). H_2O samples derived from cleaned NADP bottles yielded approximately 1.4 pg of Pb per milliliter of H_2O, which is dominantly derived from the 18.2 MΩ cm H_2O and not the NADP sample bottles. The smallest sample in our dataset gave 12-ng total Pb from 420 g of precipitation, and the procedural blanks are not significant relative to this quantity. Assuming 1/2 of the NADP bottle blank is from the bottles (0.7 pg mL^{-1}), the sampling bottle could have contributed up to ~300 pg to the sample, equating to a 2.5% blank contribution in a worst-case scenario. This information indicates that blank contamination is not responsible for any deviations or trends observed in the dataset.

References

Aarons, S. M., S. M. Aciego, and J. D. Gleason, 2013: Variable Hf–Sr–Nd radiogenic isotopic compositions in a Saharan dust storm over the Atlantic: Implications for dust flux to oceans, ice sheets and the terrestrial biosphere. *Chem. Geol.*, **349–350**, 18–26, https://doi.org/10.1016/j.chemgeo.2013.04.010.

——, M. A. Blakowski, S. M. Aciego, E. I. Stevenson, K. W. W. Sims, S. R. Scott, and C. Aarons, 2017: Geochemical characterization of critical dust source regions in the American West. *Geochim. Cosmochim. Acta*, **215**, 141–161, https://doi.org/10.1016/j.gca.2017.07.024.

Abouchami, W., and Coauthors, 2013: Geochemical and isotopic characterization of the Bodélé Depression dust source and implications for transatlantic dust transport to the Amazon basin. *Earth Planet. Sci. Lett.*, **380**, 112–123, https://doi.org/10.1016/j.epsl.2013.08.028.

Aciego, S. M., and Coauthors, 2017: Dust outpaces bedrock in nutrient supply to montane forest ecosystems. *Nat. Commun.*, **8**, 14800, https://doi.org/10.1038/ncomms14800.

Baddock, M. C., J. E. Bullard, and R. G. Bryant, 2009: Dust source identification using MODIS: A comparison of techniques applied to the Lake Eyre basin, Australia. *Remote Sens. Environ.*, **113**, 1511–1528, https://doi.org/10.1016/j.rse.2009.03.002.

Bollhöfer, A., and K. J. R. Rosman, 2000: Isotopic source signatures for atmospheric lead: The Southern Hemisphere. *Geochim. Cosmochim. Acta*, **64**, 3251–3262, https://doi.org/10.1016/S0016-7037(00)00436-1.

——, and ——, 2001: Isotopic source signatures for atmospheric lead: The Northern Hemisphere. *Geochim. Cosmochim. Acta*, **65**, 1727–1740, https://doi.org/10.1016/S0016-7037(00)00630-X.

Bory, A. J.-M., W. Abouchami, S. J. G. Galer, A. Svensson, J. N. Christensen, and P. E. Biscaye, 2014: A Chinese imprint in insoluble pollutants recently deposited in central Greenland as indicated by lead isotopes. *Environ. Sci. Technol.*, **48**, 1451–1457, https://doi.org/10.1021/es4035655.

Boyle, E. A., and Coauthors, 2014: Anthropogenic lead emissions in the ocean: The evolving global experiment. *Oceanography*, **27** (1), 69–75, https://doi.org/10.5670/oceanog.2014.10.

Callender, E., and P. C. Van Metre, 1997: Reservoir sediment cores show U.S. lead declines. *Environ. Sci. Technol.*, **31**, 424A–428A, https://doi.org/10.1021/es972473k.

Chiapello, I., G. Bergametti, B. Gomes, and B. Chatenet, 1995: An additional low layer transport of Sahelian and Saharan dust over the north-eastern tropical Atlantic. *Geophys. Res. Lett.*, **22**, 3191–3194, https://doi.org/10.1029/95GL03313.

Conway, T. M., D. S. Hamilton, R. U. Shelley, A. M. Aguilar-Islas, W. M. Landing, N. M. Mahowald, and S. G. John, 2019: Tracing and constraining anthropogenic aerosol iron fluxes to the North Atlantic Ocean using iron isotopes. *Nat. Commun.*, **10**, 2628, https://doi.org/10.1038/s41467-019-10457-w.

Duce, R. A., C. K. Unni, B. J. Ray, J. M. Prospero, and J. T. Merrill, 1980: Long-range atmospheric transport of soil dust from Asia to the tropical North Pacific: Temporal variability. *Science*, **209**, 1522–1524, https://doi.org/10.1126/science.209.4464.1522.

Eisenreich, S. J., N. A. Metzer, and N. R. Urban, 1986: Response of atmospheric lead to decreased use of lead in gasoline. *Environ. Sci. Technol.*, **20**, 171–174, https://doi.org/10.1021/es00144a010.

Erel, Y., and J. Torrent, 2010: Contribution of Saharan dust to Mediterranean soils assessed by sequential extraction and Pb and Sr isotopes. *Chem. Geol.*, **275**, 19–25, https://doi.org/10.1016/j.chemgeo.2010.04.007.

Escobar, J., T. J. Witmore, G. D. Kamenov, and M. A. Riedinger-Whitmore, 2013: Isotope record of anthropogenic lead pollution in lake sediments of Florida, USA. *J. Paleolimnol.*, **49**, 237–252, https://doi.org/10.1007/s10933-012-9671-9.

Ewing, S. A., J. S. Christensen, S. T. Brown, R. A. VanCuren, S. S. Cliff, and D. J. DePaolo, 2010: Pb isotopes as an indicator of the Asian contribution to particulate air pollution in urban California. *Environ. Sci. Technol.*, **44**, 8911–8916, https://doi.org/10.1021/es101450t.

Ganor, E., and Y. Mamane, 1982: Transport of Saharan dust across the eastern Mediterranean. *Atmos. Environ.*, **16**, 581–587, https://doi.org/10.1016/0004-6981(82)90167-6.

Goudie, A. S., 1983: Dust storms in space and time. *Prog. Phys. Geogr.*, **7**, 502–530, https://doi.org/10.1177/030913338300700402.

——, and N. J. Middleton, 2001: Saharan dust storms: Nature and consequences. *Earth-Sci. Rev.*, **56**, 179–204, https://doi.org/10.1016/S0012-8252(01)00067-8.

Graney, J. R., and M. S. Landis, 2013: Coupling meteorology, metal concentrations, and Pb isotopes for source attribution in archived precipitation samples. *Sci. Total Environ.*, **448**, 141–150, https://doi.org/10.1016/j.scitotenv.2012.07.031.

——, A. N. Halliday, G. J. Keeler, J. O. Nriagu, J. A. Robbins, and S. A. Norton, 1995: Isotopic record of lead pollution in lake sediments from the northeastern United States. *Geochim. Cosmochim. Acta*, **59**, 1715–1728, https://doi.org/10.1016/0016-7037(95)00077-D.

Grousset, F. E., and P. E. Biscaye, 2005: Tracing dust sources and transport patterns using Sr, Nd, and Pb isotopes. *Chem. Geol.*, **222**, 149–167, https://doi.org/10.1016/j.chemgeo.2005.05.006.

Hamelin, B., F. E. Grousset, P. E. Biscaye, and A. Zindler, 1989: Lead isotopes in trade wind aerosols at Barbados: The influence of European emissions over the North Atlantic. *J. Geophys. Res.*, **94**, 16 243–16 250, https://doi.org/10.1029/JC094iC11p16243.

Hart, S. R., 1984: A large-scale isotope anomaly in the Southern Hemisphere mantle. *Nature*, **309**, 753–757, https://doi.org/10.1038/309753a0.

Kamenov, G. D., M. Brenner, and J. L. Tucker, 2009: Anthropogenic versus natural control on trace element and Sr–Nd–Pb isotope stratigraphy in peat sediments of southeast Florida (USA), ~1500 AD to present. *Geochim. Cosmochim. Acta*, **73**, 3549–3567, https://doi.org/10.1016/j.gca.2009.03.017.

Kelly, A. E., M. K. Reuer, N. F. Goodkin, and E. A. Boyle, 2009: Lead concentrations and isotopes in corals and water near Bermuda, 1780–2000. *Earth Planet. Sci. Lett.*, **283**, 93–100, https://doi.org/10.1016/j.epsl.2009.03.045.

Kumar, A., W. Abouchami, S. J. G. Galer, V. H. Garrison, E. Williams, and M. O. Andreae, 2014: A radiogenic isotope tracer study of transatlantic dust transport from Africa to the Caribbean. *Atmos. Environ.*, **82**, 130–143, https://doi.org/10.1016/j.atmosenv.2013.10.021.

——, ——, ——, S. P. Singh, K. W. Fomba, J. M. Prospero, and M. O. Andreae, 2018: Seasonal radiogenic isotopic variability of the African dust outflow to the tropical Atlantic Ocean and across to the Caribbean. *Earth Planet. Sci. Lett.*, **487**, 94–105, https://doi.org/10.1016/j.epsl.2018.01.025.

Muhs, D. R., C. A. Bush, K. C. Stewarts, T. R. Rowland, and R. C. Crittenden, 1990: Geochemical evidence of Saharan dust parent material for soils developed on quaternary limestones of Caribbean and western Atlantic islands. *Quat. Res.*, **33**, 157–177, https://doi.org/10.1016/0033-5894(90)90016-E.

Perry, K. D., T. A. Cahill, R. A. Eldred, and D. Dutcher, 1997: Long-range transport of North African dust to the eastern United States. *J. Geophys. Res.*, **102**, 11 225–11 238, https://doi.org/10.1029/97JD00260.

Petit, J.-R., M. Briat, and A. Royer, 1981: Ice Age aerosol content from East Antarctic ice core samples and past wind strength. *Nature*, **293**, 391–394, https://doi.org/10.1038/293391a0.

Prospero, J. M., and T. N. Carlson, 1972: Vertical and areal distribution of Saharan dust over the western equatorial North Atlantic Ocean. *J. Geophys. Res.*, **77**, 5255–5265, https://doi.org/10.1029/JC077i027p05255.

Rayegani, B., S. Barati, H. Goshtasb, S. Gachpaz, J. Ramezani, and H. Sarkheil, 2020: Sand and dust storm sources identification: A remote sensing approach. *Ecol. Indic.*, **112**, 106099, https://doi.org/10.1016/j.ecolind.2020.106099.

Sassen, K., 2002: Indirect climate forcing over the western US from Asian dust storms. *Geophys. Res. Lett.*, **29**, 1465, https://doi.org/10.1029/2001GL014051.

Schütz, L., and M. Sebert, 1987: Mineral aerosols and source identification. *J. Aerosol Sci.*, **18**, 1–10, https://doi.org/10.1016/0021-8502(87)90002-4.

Scott, S. R., and Coauthors, 2019: The application of abundance sensitivity filters to the precise and accurate measurement of uranium series nuclides

by plasma mass spectrometry. *Int. J. Mass Spectrom.*, **435**, 321–332, https://doi.org/10.1016/j.ijms.2018.11.011.

Settle, D. M., C. C. Patterson, K. K. Turekian, and J. K. Cochran, 1982: Lead precipitation fluxes at tropical ocean sites determined from ^{210}Pb measurements. *J. Geophys. Res.*, **87**, 1239–1245, https://doi.org/10.1029/JC087iC02p01239.

Sherman, L. S., J. D. Blum, J. T. Dvonch, L. E. Gratz, and M. S. Landis, 2015: The use of Pb, Sr, and Hg isotopes in Great Lakes precipitation as a tool for pollution source attribution. *Sci. Total Environ.*, **502**, 362–374, https://doi.org/10.1016/j.scitotenv.2014.09.034.

Shirahata, H., R. W. Elias, C. C. Patterson, and M. Koide, 1980: Chronological variations in concentrations and isotopic compositions of anthropogenic atmospheric lead in sediments of a remote subalpine pond. *Geochim. Cosmochim*. Acta, **44**, 149–162, https://doi.org/10.1016/0016-7037(80)90127-1.

Simonetti, A., C. Gariépy, and J. Carignan, 2000a: Pb and Sr isotopic compositions of snowpack from Québec, Canada: Inferences on the sources and deposition budgets of atmospheric heavy metals. *Geochim. Cosmochim. Acta*, **64**, 5–20, https://doi.org/10.1016/S0016-7037(99)00207-0.

——, ——, and ——, 2000b: Pb and Sr isotopic evidence for sources of atmospheric heavy metals and their deposition budgets in northeastern North America. *Geochim. Cosmochim. Acta*, **64**, 3439–3452, https://doi.org/10.1016/S0016-7037(00)00446-4.

Strelow, F. W. E., and F. V. S. Toerien, 1966: Separation of lead(II), from bismuth(III), thallium(III), cadmium(II), mercury(II), gold(III), platinium(IV), palladium(II), and other elements by anion exchange chromatography. *Anal. Chem*., **38**, 545–548, https://doi.org/10.1021/ac60236a006.

Swap, R., M. Garstang, and S. Greco, 1992: Saharan dust in the Amazon basin. *Tellus*, **44B**, 133–149, https://doi.org/10.3402/tellusb.v44i2.15434.

Tegen, I., M. Werner, S. P. Harrison, and K. E. Kohfeld, 2004: Relative importance of climate and land use in determining present and future global soil dust emission. *Geophys. Res. Lett.*, **31**, L05105, https://doi.org/10.1029/2003GL019216.

Thirlwall, M. F., 2002: Multicollector ICP-MS analysis of Pb isotopes using a 207pb-204pb double spike demonstrates up to 400 ppm/amu systematic errors in Tl-normalization. *Chem. Geol.*, **184**, 255–279, https://doi.org/10.1016/S0009-2541(01)00365-5.

Torfstein, A., and Coauthors, 2017: Chemical characterization of atmospheric dust from a weekly time series in the north Red Sea between 2006 and 2010. *Geochim. Cosmochim. Acta*, **211**, 373–393, https://doi.org/10.1016/j.gca.2017.06.007.

Washington, R., M. Todd, N. J. Middleton, and A. S. Goudie, 2003: Dust-storm source areas determined by the total ozone monitoring spectrometer and surface observations. *Ann. Assoc. Amer. Geogr.*, **93**, 297–313, https://doi.org/10.1111/1467-8306.9302003.

Wetherbee, G. A., D. A. Gay, T. M. Debey, C. M. B. Lehmann, and M. A. Nilles, 2012: Wet deposition of fission-product isotopes to North America from the Fukushima Dai-ichi incident, March 2011. *Environ. Sci. Technol.*, **46**, 2574–2582, https://doi.org/10.1021/es203217u.

Yu, H., and Coauthors, 2015: The fertilizing role of African dust in the Amazon rainforest: A first multiyear assessment based on data from Cloud-Aerosol Lidar and Infrared Pathfinder Satellite Observations. *Geophys. Res. Lett.*, **42**, 1984–1991, https://doi.org/10.1002/2015GL063040.

Zurbrick, C. M., and Coauthors, 2018: Dissolved Pb and Pb isotopes in the North Atlantic from the GEOVIDE transect (GEOTRACES GA-01) and their decadal evolution. *Biogeosciences*, **15**, 4995–5014, https://doi.org/10.5194/bg-15-4995-2018.